# Upstream effect on the upper dome of SMR structures

Suyeon Park <sup>a</sup>, Bum Jin Chung <sup>a\*</sup>
<sup>a</sup>Kyunghee university, Gyeonggi-do, Yongin-si, Giheung-gu, Deogyeong-daero 1732
\*Corresponding author: bjchung@khu.ac.kr

\*Keywords: Dome, Upstream effect, SMR, Flow visualization

# 1. Introduction

Small modular reactors (SMRs) have been receiving increasing attention due to their favorable economics. They enable the deployment of nuclear reactors beyond national-scale applications, and an increasing number of companies and considering SMRs to meet their electricity demands.

In response to increased nuclear safety requirements, several SMR designs have adopted passive cooling systems for use during severe accidents. Although SMRs are smaller in size compared to conventional nuclear power plants, they are still large in scale with respect to natural heat transfer phenomena. This study focuses on the upper dome of the containment vessel (CV), which is the region most exposed to vapor in the event of a loss-of-coolant-accident (LOCA) [1-3]. This indicates that natural convection around the dome plays a critical role in maintaining reactor integrity. If sufficient cooling is provided, vapor condensation on the dome surface can contribute to pressure reduction within the CV.

The diameter of licensed or currently designed SMRs, such as Westinghouse at 9.75 m and NuScale's VOYGR at 4.6m, generally range between 4 to 10 m [4]. Their scale as Rayleigh number ( $Ra_{Db}$ ) is over  $10^9$  while the study about natural convection around the dome shape were covered below 10<sup>9</sup> [5-8]. In our previous study, we investigated external natural convection around the dome across a wide range of Rayleigh numbers  $(Ra_{Db})$  and for various dome geometrical characteristic factor, truncation angle  $(\theta)$  with domeonly heating conditions [9]. Truncation angle is the angle from the leading edge of the dome to the apex of the dome and as it decrease, the dome shape getting close to the flat plate. The average Nusselt number  $(Nu_{Db})$  was found to decrease with smaller truncation angles, and the decreasing trend became less significant at higher  $Ra_{Db}$ .

However, the dome does not exist in isolation; it is connected to a heated cylindrical section beneath it, which influences the incoming flow toward the dome. In the present study, we experimentally examine the effects of varying truncation angles  $(\theta)$  and upstream cylinder heights on the external natural convection heat transfer around the dome. The results provide insight into how upstream flow conditions affect the overall heat transfer performance in passive cooling scenarios.

## 2. Experimental method

### 2.1 Mass transfer method

In this experiments, heat transfer experiments will be substituted with mass transfer experiments using the analogy concept [10]. The governing equations for heat and mass transfer are analogous and belong to the same mathematical class. In heat transfer system, temperature (T) and thermal diffusivity ( $\alpha$ ) can be directly compared to concentration (C) and mass diffusivity  $(D_m)$  in mass transfer systems. In this study, a CuSO<sub>4</sub>-H2SO<sub>4</sub> copper electroplating system was chosen. When an electric potential is applied to electrodes submerged in a CuSO<sub>4</sub>-H<sub>2</sub>SO<sub>4</sub> aqueous solution and are subsequently reduced at the cathode. The concentration between the cathode surface and the bulk fluid is analogous to the temperature difference between the heater surface and the bulk fluid, while the current density represents the heat flux. However, accurately measuring the concentration of cupric ions at the cathode surface during mass transfer experiments is challenging, so the limit current technique is employed [11].

This experimental technique, based on the heat and mass transfer analogy, has been employed by various researchers [12, 13]. Typically,  $D_m$  is much smaller than  $\alpha$ , making mass transfer systems particularly suitable for simulating fluids with high Prandtl numbers. This system is effective in achieving high  $Ra_{Db}$ . Table 1 presents the corresponding governing parameters for both heat and mass transfer systems. The mass transfer coefficient (hm) can be obtained by Eq. (1). In this context, the amount of copper ions deposited on the cathode is analogous to the amount of heat transfer. Consequently, the observed electroplating patterns serves as a representation of the local heat transfer patterns [14].

$$h_m = \frac{(1 - t_n)I_{\lim}}{nFC_b} \tag{1}$$

Table I. Dimensionless numbers for the analogous systems.

Heat transfer		Mass transfer	
Nu	$h_hD/k$	Sh	$h_mD/D_m$
Pr	$\nu/\alpha$	Sc	$v/D_m$
$Ra_{Db}$	$g\beta\Delta TD_b^3/\alpha v$	$Ra_{Db}$	$GD_b^3/D_m v$

# 2.2 Test matrix and rig

Table II shows test matrix. The Pr was fixed at 2094. Additionally, Base diameter ( $D_b$ ) and the corresponding  $Ra_{Db}$  was set to the minimum scale of SMRs. Fig. 1 shows the simple description of the geometrical factors composing dome. Base diameter of the dome is equal to the diameter of cylinder beneath the dome. Dome as the partial structure of sphere, truncation angle is the polar angle between the leading edge of the dome and the apex of it. Two extreme  $\theta$  were selected, and a test matrix ranging from 0.05 to 0.25 cm in upstream height was established to observe the heat transfer characteristics of the dome as the upstream height increased..

Table II. Test matrix

Pr	$D_b$ (m)	$Ra_{Db}$	θ (°)	H(m)
2094	0.1	1.68 ×10 <sup>11</sup>	30, 90	0.05, 0.10, 0.15, 0.20, 0.25

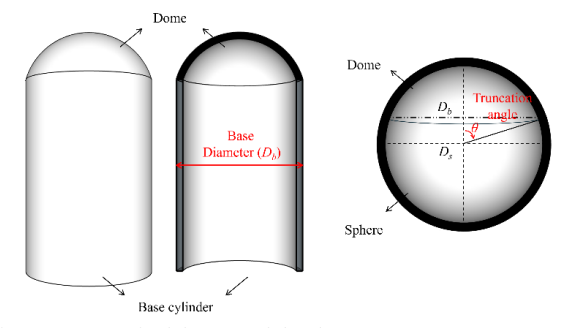


Fig. 1. Geometrical factors of the dome concept.

Figure 2 shows the schematic image of the experimental apparatus along with its electrical circuit diagram. A dome shape cathode and cylindrical cathode was placed at the center of an acrylic tank. The cathode was sectioned to observed the variation in heat transfer according to the fluid flow. Four rectangular anodes located at each sides of the acrylic tank walls to ensure stable electrical current. Power was supplied through a power source (Vüpower K1810), and current was measured and recorded using a DAQ (NI9227).

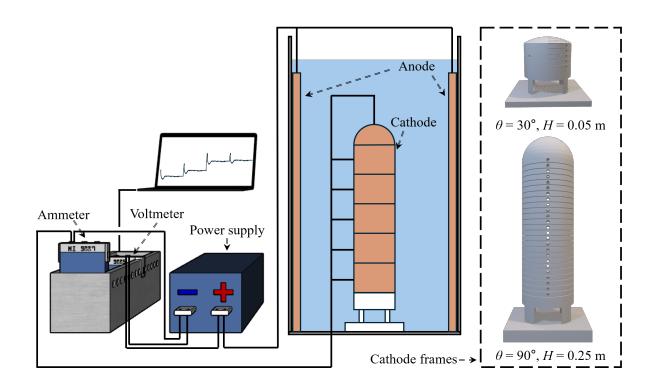


Fig. 2. Diagram of the experimental apparatus with electrical circuit diagram.

### 3. Result and discussion

#### 3.1 Experimental validation

To verify the validity of the experimental results, comparison with the correlation for upper dome only correlation proposed by Park et al. (2025) [9]. Fig. 3 shows the measured  $Nu_{Db}$  for  $\theta = 90^{\circ}$  and 30° with the correlation. The difference with measured  $Nu_{Db}$  and correlation are 4.8% and 0.7 % for each  $\theta = 90^{\circ}$  and 30°.

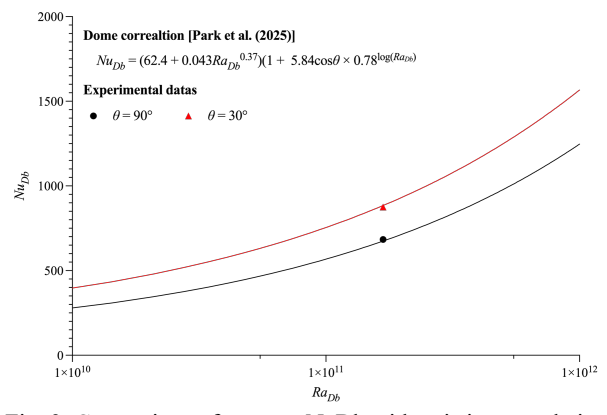


Fig. 3. Comparison of average NuDb with existing correlation.

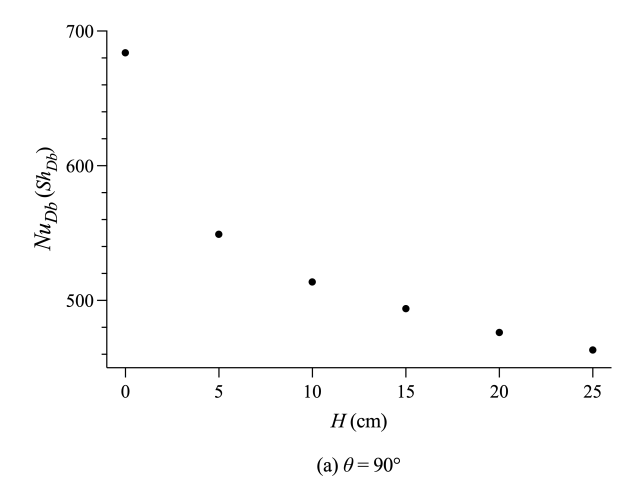
With using piecewise electrodes to measure the local value, loss of cathode area to insulate was inevitable. Average loosen area are 5.92 cm<sup>2</sup> and 3.13 cm<sup>2</sup> for each dome with  $\theta = 90^{\circ}$  and 30°. Loosen limiting current by using piecewise cathode is 1.44% compared to the 1/4 sized piecewise cathode ( $\sum I_{lim, \sum piecewise}$  /  $I_{lim, quarter} = 0.9856$ ) which is negligible.

# 3.2 Average Nudb with Increasing Upstream Height

Figure 4 shows the average  $Nu_{Db}$  of the dome for entire experimental cases. For both truncation angle cases,  $Nu_{Db}$  decreases as the upstream height increases. Most distinct difference came from the existence of upstream. Dome heat transfer decrease about 14.5% and 19.7% for each  $\theta = 90^{\circ}$  and  $30^{\circ}$  cases as upstream exist (H = 5 cm).

Average  $Nu_{Db}$  keep decrease as the upstream height increase, in  $\theta = 90^{\circ}$  case,  $Nu_{Db,H=25}$  diminish until 0.68  $Nu_{Db,H=0}$ . The width of decrease as H increase decrease exponentially and it seemed like going to converge after H=25 cm.

Unlike  $\theta = 90^{\circ}$  case,  $Nu_{Db,H=25}$  diminish until 0.73  $Nu_{Db,H=0}$  in  $\theta = 30^{\circ}$  case.  $Nu_{Db}$  decrease smaller than  $\theta = 90^{\circ}$  case. Also,  $Nu_{Db}$  of  $\theta = 30^{\circ}$  case doesn't decrease exponentially, rather it had simillar width of decrease as H increase.



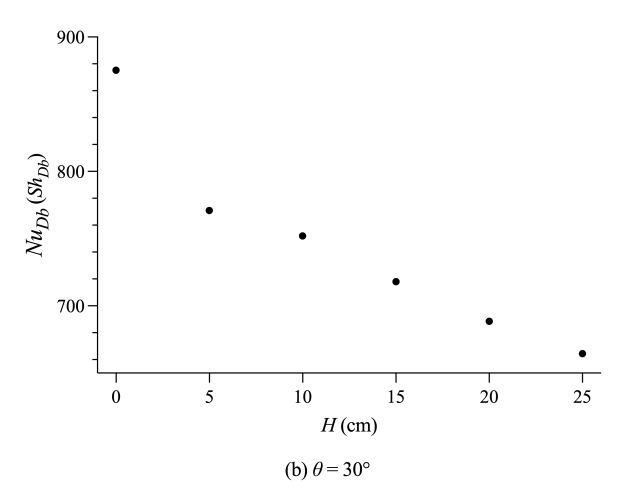


Fig. 4. Average  $Nu_{Db}$  of dome only case (H = 0) with various upstream height.

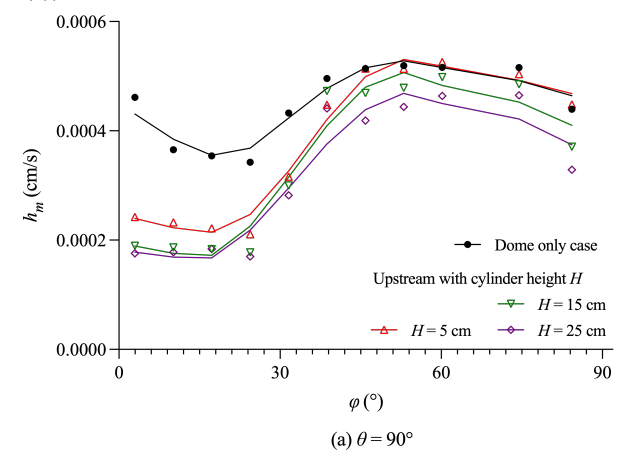
# 3.2 Local h<sub>m</sub> of dome with upstream

Average  $Nu_{Db}$  of the dome decrease as the upstream exist and its height increase. To confirm the local thermal behavior around the dome, local  $h_m$  were measured using piecewise cathode. Fig. 5 shows the local  $h_m$  according to the position of measurement, expressed using polar angle  $(\varphi)$ .  $\varphi = 0^\circ$  at leading edge and  $\varphi = \theta$  at the apex.

Both  $\theta = 90^{\circ}$  and  $30^{\circ}$  cases, local  $h_m$  of upstream cases near the leading edge definitely decrease compared to the dome only case. This is due to the preheating effect. For the dome only case, fresh fluid supplied to the leading edge of the dome and high heat transfer occurs. However, as the upstream exist, fluid which already heated from upstream enter the leading edge of dome so no more leading edge effect occurs at the start position of the dome. As the  $h_m$  measurement, it can confirm that the effect of upstream existence is highly depends on the extinction of leading edge effect.

Local  $h_m$  for upstream cases decreases compared to the dome only existence case but their overview of the  $h_m$  are quite similar nevertheless of upstream existence

and its height. Local  $h_m$  increase near the  $\varphi = 30^\circ$  and measured similar after the point only with little different of the absolute value for entire cases of  $\theta = 90^\circ$  (Fig. 5 (a)).



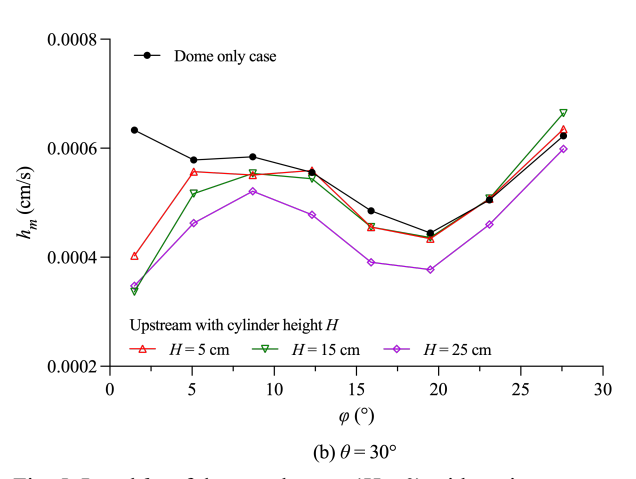


Fig. 5. Local  $h_m$  of dome only case (H = 0) with various upstream height.

 $\theta = 30^{\circ}$  dome also has similar effect of upstream with  $\theta = 90^{\circ}$ , but quite short effect of leading edge extinction was observed (Fig. 5(b)).  $h_{\rm m}$  of the upstream existence case of  $\theta = 90^{\circ}$  case join the similar thermal behavior after  $\varphi > \theta / 3$  but only after  $\varphi > \theta / 6$  for  $\theta = 30^{\circ}$  case.

# 3. Conclusions

We investigated the heat transfer characteristics of domes with two extreme truncation angle,  $\theta=90^{\circ}$  and  $30^{\circ}$ , while gradually increasing the upstream height. The observations revealed that when the upstream was present (the case with the smallest H), the largest heat transfer loss occurred, and as the upstream height increased, the heat transfer loss of the dome also increased. Local heat transfer measurements confirmed that the most significant influence of the upstream on the dome's heat transfer was the extinction of the leading-edge effect. Furthermore, it was observed that, beyond this point, the thermal behavior of the dome became similar regardless of whether the upstream was

present or absent. This suggest that the flow entering the dome from the upstream does not significantly alter the natural convection pattern compared to the isolated dome case, but rather sustains it. To further validate this inference, further work is planned to include flow visualization using particle image velocimetry and additional experiments with a wider range of truncation angles and  $Ra_{Db}$ .

# **ACKNOLEDGMENTS**

This work was supported by the Innovative Small Modular Reactor Development Agency grant funded by the Korea Government (MOTIE) (No. RS-2024-00404240).

This study was also sponsored by the Ministry of Science and ICT (MSIT) and was supported by nuclear Research & Development program grant funded by the National Research Foundation (NRF) (No. RS-2025-02653218).

#### REFERENCES

- [1] E.M.A. Hussein, Emerging small modular nuclear power reactors: A critical review, Physics Open, 5 (2020).
- [2] Z. Liu, J. Fan, Technology readiness assessment of Small Modular Reactor (SMR) designs, Progress in Nuclear Energy, 70 (2014) 20-28.
- [3] M. Santinello, M. Ricotti, Long-term decay heat removal in a submerged SMR, Annals of Nuclear Energy, 131 (2019) 39-50.
- [4] A. International Atomic Energy, Advances in Small Modular Reactor Technology Developments A Supplement to: IAEA Advanced Reactors Information System (ARIS) 2020 Edition, in, International Atomic Energy Agency (IAEA), 2020, pp. 354.
- [5] Y. Jaluria, B. Gebhart, On the buoyancy-induced flow arising from a heated hemisphere, International Journal of Heat and Mass Transfer, 18 (1975) 415-431.
- [6] J. Liu, C.-J. Zhao, H. Liu, W.-Q. Lu, Numerical study of laminar natural convection heat transfer from a hemisphere with adiabatic plane and isothermal hemispherical surface, International Journal of Thermal Sciences, 131 (2018) 132-143.
- [7] S. Acharya, Natural Convection Heat Transfer from Upward, Downward, and Sideward Solid/Hollow Hemispheres, Journal of Thermophysics and Heat Transfer, 36 (2022) 141-153.
- [8] C. Dong, S. Chen, R. Chen, W. Tian, S. Qiu, G.H. Su, Numerical simulation of natural convection around the dome in the passive containment air-cooling system, Nuclear Engineering and Technology, 55 (2023) 2997-3009.
- [9] S.-Y. Park, D.-H. Park, B.-J. Chung, Natural convection experiments around an upper dome varying Rayleigh number and truncation angle, Experimental Thermal and Fluid Science, 169 (2025) 111548.

- [10] A. Bejan, Mass Transfer, in: Convection Heat Transfer, 2013, pp. 489-536.
- [11] S.-H. Ko, D.-W. Moon, B.-J. Chung, Applications of electroplating method for heat transfer studies using analogy concept, Nuclear Engineering and Technology, 38 (2006).
- [12] D.W. Hubbard, E.N. Lightfoot, Correlation of Heat and Mass Transfer Data for High Schmidt and Reynolds Numbers, Industrial & Engineering Chemistry Fundamentals, 5 (1966) 370-379.
- [13] F.P. Berger, K.F.F.L. Hau, Mass transfer in turbulent pipe flow measured by the electrochemical method, International Journal of Heat and Mass Transfer, 20 (1977) 1185-1194.
- [14] B.-J. Chung, J.-H. Eoh, J.-H. Heo, Visualization of natural convection heat transfer on horizontal cylinders, Heat and Mass Transfer, 47 (2011) 1445-1452.